Geophysical Research Letters

RESEARCH LETTER
10.1029/2022GL100218

Preferential Formation of Chlorite Over Talc During Si-Metasomatism of Ultramafic Rocks in Subduction Zones

E. A. Codillo[1,2], F. Klein[3], and H. R. Marschall[2,4]

[1]Massachusetts Institute of Technology/Woods Hole Oceanographic Institution Joint Program in Oceanography/Applied Ocean Science and Engineering, Woods Hole, MA, USA, [2]Department of Geology and Geophysics, Woods Hole Oceanographic Institution, Woods Hole, MA, USA, [3]Department of Marine Chemistry and Geochemistry, Woods Hole Oceanographic Institution, Woods Hole, MA, USA, [4]Institut für Geowissenschaften, Goethe Universität Frankfurt, Frankfurt am Main, Germany

Key Points:

- Limited talc formation by Si-metasomatism of ultramafic rocks in subduction zones
- Chlorite formation is likely pervasive at the slab-mantle interface
- Preferential formation of chlorite has wide-ranging chemical and physical implications for subduction zone processes

Supporting Information:

Supporting Information may be found in the online version of this article.

Correspondence to:

E. A. Codillo,
ecodillo@mit.edu

Citation:

Codillo, E. A., Klein, F., & Marschall, H. R. (2022). Preferential formation of chlorite over talc during Si-metasomatism of ultramafic rocks in subduction zones. *Geophysical Research Letters*, *49*, e2022GL100218. https://doi.org/10.1029/2022GL100218

Received 27 JUN 2022
Accepted 19 SEP 2022

Author Contributions:

Conceptualization: E. A. Codillo, F. Klein
Formal analysis: E. A. Codillo, F. Klein, H. R. Marschall
Funding acquisition: F. Klein, H. R. Marschall
Investigation: E. A. Codillo, F. Klein, H. R. Marschall
Methodology: E. A. Codillo, F. Klein
Project Administration: F. Klein, H. R. Marschall
Supervision: F. Klein, H. R. Marschall
Validation: E. A. Codillo
Visualization: E. A. Codillo
Writing – original draft: E. A. Codillo
Writing – review & editing: E. A. Codillo, F. Klein, H. R. Marschall

Abstract Talc formation via silica-metasomatism of ultramafic rocks is believed to play key roles in subduction zone processes. Yet, the conditions of talc formation remain poorly constrained. We used thermodynamic reaction-path models to assess the formation of talc at the slab-mantle interface and show that it is restricted to a limited set of pressure–temperature conditions, protolith, and fluid compositions. In contrast, our models predict that chlorite formation is ubiquitous at conditions relevant to the slab-mantle interface of subduction zones. The scarcity of talc and abundance of chlorite is evident in the rock record of exhumed subduction zone terranes. Talc formation during Si-metasomatism may thus play a more limited role in volatile cycling, strain localization, and in controlling the decoupling-coupling transition of the plate interface. Conversely, the observed and predicted ubiquity of chlorite corroborates its prominent role in slab-mantle interface processes that previous studies attributed to talc.

Plain Language Summary In subduction zones, talc can form during chemical reactions of mantle rocks with silica-enriched fluids at the interface between descending oceanic plates and the overriding mantle. Its formation and distribution in subduction zones are believed to affect the volatile budget, rheological properties, and the down-dip limit of the decoupling of the slab-mantle interface. Therefore, illuminating the conditions that facilitate talc formation at high pressure-temperature conditions is key in assessing its roles in fundamental subduction zone processes. Using thermodynamic reaction-path models, we show that the formation of talc at the slab-mantle interface is restricted to a limited set of environmental conditions, because its formation is highly sensitive to the compositions of the mantle rocks and reactant fluids. Contrary to common belief, talc is unlikely to form in high abundance in ultramafic rocks metasomatized by Si-rich slab-derived fluids. Rather, our models predict the ubiquitous formation of chlorite along with other silicate minerals during Si-metasomatism due to the competing effects from other dissolved components that favor their formation over talc. This study calls into question the importance of talc during Si-metasomatism in subduction zones but highlights the more predominant role of chlorite.

1. Introduction

Talc [$(Mg,Fe)_3Si_4O_{10}(OH)_2$] is a hydrous phyllosilicate, which forms at the expense of ultramafic rocks in the oceanic crust, orogenic belts, and subduction zones (Boschi et al., 2006; S. M. Peacock and Hyndman, 1999). It contains ∼5 wt.% water and can be stable to high temperatures (T) and pressures (P), suggesting that it is a potentially important mineral in the global water cycle (Bebout, 1991; Bose & Ganguly, 1995; S. Peacock, 1990). In wet conditions, talc is mechanically weak and can localize shear stress, thus affecting the rheological and seismogenic properties of faults and plate boundaries (Chen et al., 2017; Hirauchi et al., 2013, 2020; Moore & Lockner, 2007).

In subduction zones, pervasive mechanical mixing of sediments, mafic, and ultramafic rocks (Bebout, 2013; Bebout and Barton, 2002; Bebout & Penniston-Dorland, 2016) facilitates metasomatism which can favor talc formation (Manning, 1995; S. M. Peacock and Hyndman, 1999). Talc can form in high-pressure ultramafic rocks that have been enriched in SiO_2 through the reaction with silica-bearing aqueous fluids (Manning, 1995, 1997). Based on geophysical data, a ∼4 km thick layer of altered ultramafic rock enriched in talc was inferred to be present at the slab-mantle interface in the central Mexican subduction zone (Kim et al., 2013).

Rheological contrasts between juxtaposed lithologies lead to strain partitioning and fluid flow along lithological boundaries further promoting metasomatic reactions (Ague, 2007). Previous laboratory friction experiments have shown that wet talc can be substantially weaker than antigorite, chlorite, and other hydrous minerals (Chen et al., 2017; Hirauchi et al., 2013, 2020; Moore & Lockner, 2007), which would promote mechanical weakening and decoupling of the slab-mantle interface (Abers et al., 2020; Marschall & Schumacher, 2012; Wada et al., 2008). The changes in the rheological properties and stress states of materials along the plate interface may manifest themselves as seismicity, such as slow slip events (Beroza & Ide, 2011; Rubin, 2008). The pressure-sensitive breakdown of talc into secondary mineral assemblage has recently been suggested to control the extent of mechanical coupling along the plate interface (S. M. Peacock and Wang, 2021). Therefore, illuminating the conditions that facilitate talc formation at high *P-T* conditions is important in assessing its importance in plate interface processes.

Metamorphosed siliceous and pelitic sediments, as well as basaltic crustal rocks commonly contain quartz, and fluids in equilibrium with these rocks are quartz saturated or even super-saturated (Hacker et al., 2003; C. E. Manning, 1995). While fluids in equilibrium with subducted metabasalt and metapelite likely exhibit elevated silica activity, the presence of other silicate minerals (e.g., kyanite, garnet, paragonite, chlorite, epidote minerals) coexisting with quartz would also affect the speciation of other dissolved major elements (e.g., Al, Mg, Ca, and Fe). The elevated *P-T* conditions in subduction zones are also expected to enhance the solubilities of dissolved elements through the formation of aqueous complexes (Manning, 2004, 2007; Sverjensky et al., 2014), which can directly affect metasomatic processes. However, such effects have remained understudied as the dielectric constant of water at pressures higher than 0.5 GPa was poorly constrained (Helgeson et al., 1981; Shock et al., 1992). The recent development of the Deep Earth Water (DEW) model allows for the prediction of the equilibrium constants of reactions to model fluid-rock interactions at high *P-T* conditions relevant to subduction zones (Huang & Sverjensky, 2019; Sverjensky, 2019; Sverjensky et al., 2014).

We used thermodynamic reaction path models to evaluate the successions of metasomatic reactions between ultramafic rocks and fluids previously equilibrated with metapelite or metabasalt over a range of *P-T* conditions relevant to slab-top geotherms of subduction zones. We compare our predictions with exhumed metamorphic rock record with known *P-T* histories. We discuss the petrological controls on talc and chlorite formation and highlight the implications of slab-derived fluid metasomatism of ultramafic rocks in subduction zones.

2. Methods

Thermodynamic reaction path models were set up to assess changes in mineralogy and fluid composition during Si-metasomatism of ultramafic rocks. Fluids equilibrated with metamorphosed mid-ocean ridge basalt (MORB) or a metapelite were subsequently allowed to react with ultramafic rocks at subduction zone conditions. To evaluate the effects of ultramafic protolith compositions on reaction pathways, we used monomineralic antigorite [$Mg_{48}Si_{34}O_{85}(OH)_{62}$], lherzolite (depleted MORB mantle, DMM), harzburgite (HZ1), and a more refractory harzburgite (HZ2) (Table S1 in Supporting Information S1). Models were calculated over a range of *P-T* conditions (1–2.5 GPa, 300°C–600°C), and a range of fluid-to-rock (f/*r*) mass ratios, using the EQ3/6 software package version 6 (Wolery, 1992) and DEW database (Huang & Sverjensky, 2019; Sverjensky et al., 2014). The reaction-path portrays a system that is initially fluid-dominated, such as in a fracture or vein, but then becomes increasingly rock-dominated as more ultramafic rock is added, such as in the rock matrix adjacent to a fracture or vein. We explored a range of f/*r* (i.e., f/*r* >> 1) to simulate conditions likely relevant to high permeability zones, such as along lithologic contacts and shear zones (Codillo, 2022). We also calculated reaction-path models to investigate the metasomatism of ultramafic rocks by fluids that previously equilibrated with quartz only (i.e., compositions of other dissolved elements are set to trace concentrations). Details on the reaction-path model setup are provided in Supporting Information S1.

3. Results

3.1. Predicted Compositions of Fluids in Equilibrium With Metabasalt, Metapelite, or Quartz

The Si concentration of a quartz-saturated fluid is predicted to increase steadily with increasing temperature and pressure. However, pressure appears to have a limited effect on the fluid composition when compared with changes in temperature. The concentrations of dissolved Mg, Si, and Al in equilibrium with metabasalt are

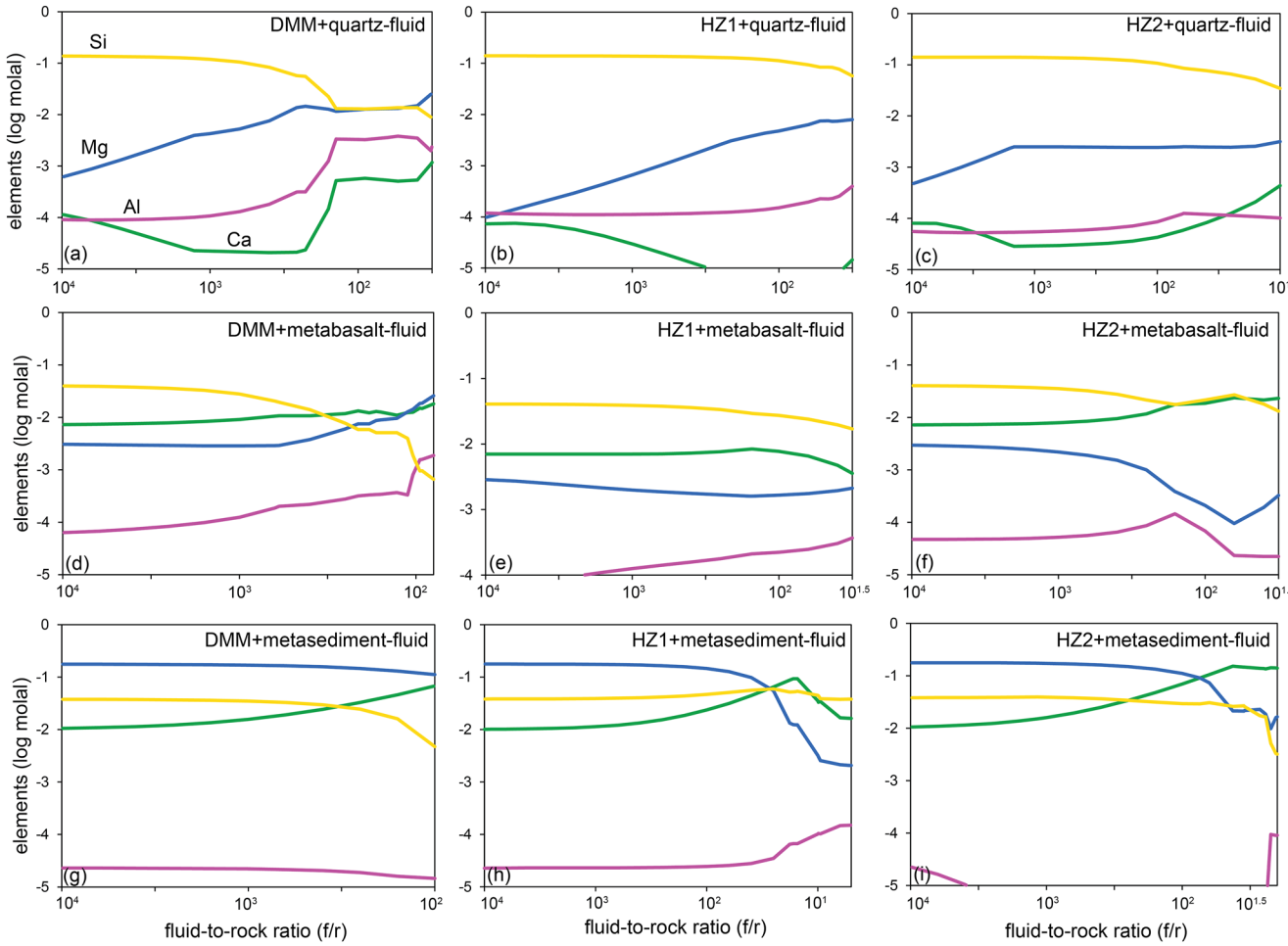

Figure 1. Predicted pore fluid composition during high *P-T* (300°C, 1.5 GPa) Si-metasomatism of ultramafic rocks as a function of fluid-to-rock ratio. A fluid equilibrated with quartz (a–c), metabasalt (d–f), or metasediments (g–i) is subsequently allowed to react with ultramafic compositions (DMM, HZ1, and HZ2). The f/*r* decreases as ultramafic rock is titrated into the fluid.

predicted to increase steadily with increasing temperature while the concentration of dissolved Ca shows no systematic trends in response to changes in temperature (Figure S1 and Table S2 in Supporting Information S1). The concentrations of dissolved Al and Si in equilibrium with metapelite are predicted to increase with increasing temperature. The concentration of dissolved Mg is predicted to decrease with increasing temperature from 300°C to 400°C, and then slightly increase between 500°C and 600°C.

3.2. Modeled Metasomatism of Ultramafic Rocks

To illustrate the effects of *P*, *T*, rock and fluid compositions on the metasomatic formation of talc, representative model results at 300°C and 1.5 GPa are presented in Figures 1, 1, and S2 in Supporting Information S1. In addition, the predicted mineral assemblages of reaction-path models that simulated Si-metasomatism at higher temperatures (400°C–600°C) at 1.5 GPa are shown in Figures S3–S5 in Supporting Information S1. All model results, including those for higher pressures, are available in the data repository. Models simulating the reaction of quartz-saturated fluid with antigorite predicted the formation of talc coexisting with quartz at all modeled *P-T* conditions (Table S3 in Supporting Information S1). At 300°C and 1.5 GPa, metasomatism of DMM lherzolite is predicted to result in the formation of talc, clinopyroxene, and chlorite. At similar *P-T* condition, our models suggests the formation of talc together with clinopyroxene + orthopyroxene + chlorite in the reaction between quartz-saturated fluid and a harzburgite (HZ1). Over the modeled conditions, metasomatism of DMM lherzolite by a quartz-saturated fluid predicted talc formation from 1.5 to 2.5 GPa, from 300 to up to 600°C (Table S3 in

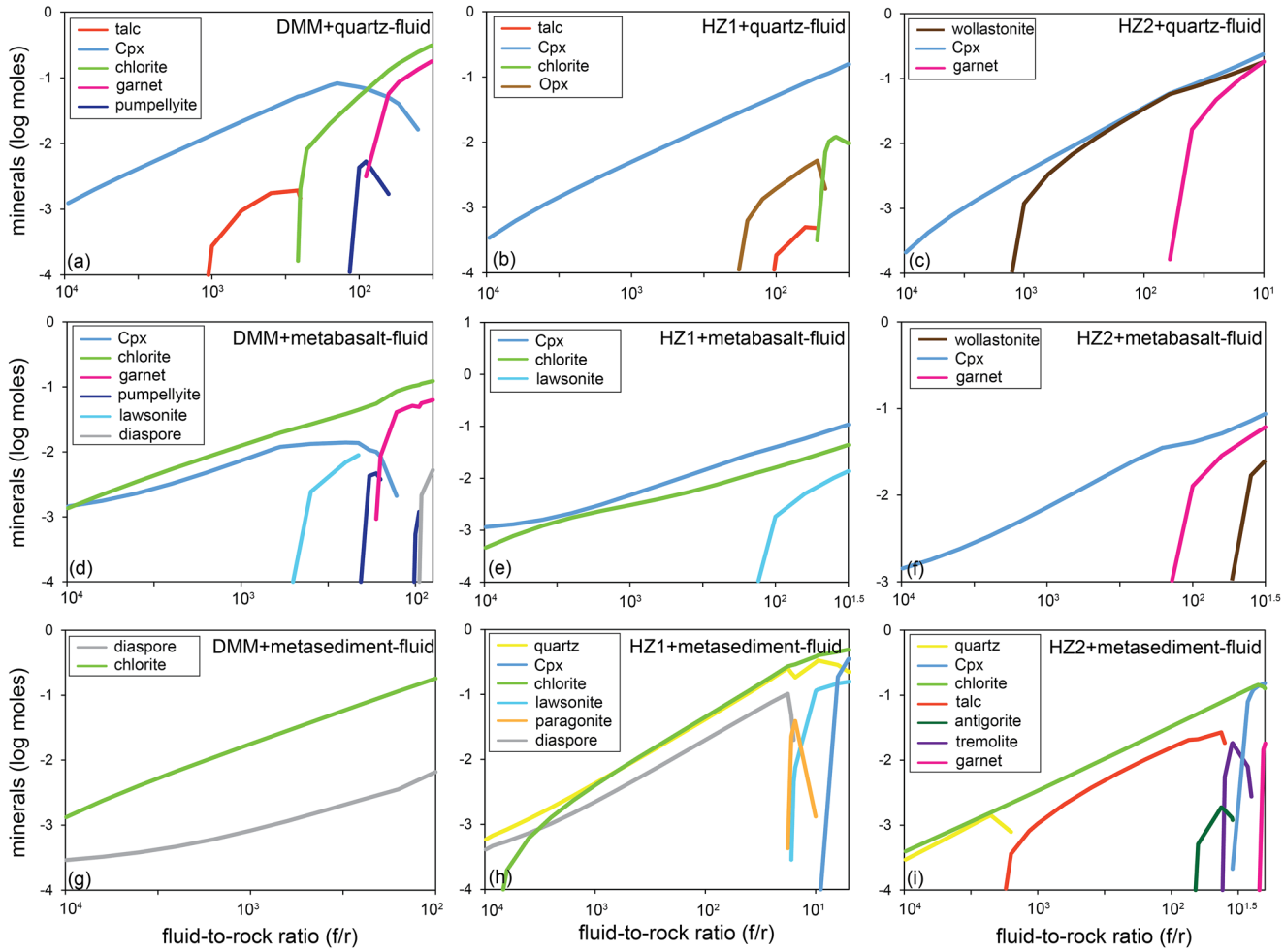

Figure 2. Predicted mineral assemblages of reaction-path models that simulated high *P-T* (300°C, 1.5 GPa) metasomatism as a function of fluid-to-rock ratio. A fluid equilibrated with quartz (a–c), metabasalt (d–f), or metasediments (g–i) is subsequently allowed to react with ultramafic compositions (DMM, HZ1, and HZ2). The f/*r* decreases as ultramafic rock is titrated into the fluid. Mineral abbreviations are from Whitney and Evans (2010).

Supporting Information S1). Metasomatism of HZ1 by a quartz-saturated fluid also predicted talc formation but at lower temperature (≤400°C) compared with reaction with DMM. In contrast, talc is not predicted to form during metasomatism of the more refractory harzburgite (HZ2) in any of the modeled conditions (Table S3 in Supporting Information S1). In general, the predicted concentrations of dissolved Mg and Al increase, dissolved Si concentrations decrease, while dissolved Ca concentrations initially decrease then increase with decreasing f/*r* (Figure 1).

Metasomatism of antigorite by fluids previously in equilibrium with a metabasalt is predicted to form talc coexisting with chlorite + clinopyroxene (diopside) + olivine at 300°C and 1.5 GPa (Figure S2 in Supporting Information S1). However, under the same *P-T* condition, talc is not predicted to form during metasomatism of DMM, HZ1, and HZ2. Instead, the models suggest the formation of Ca and Al-bearing minerals such as clinopyroxene, chlorite, garnet, pumpellyite, wollastonite, and diaspore (Figures 2d–2f). Our models predict that metasomatism of DMM, HZ1, and HZ2 by fluids that previously equilibrated with metabasalt yields talc over a narrow range of *P-T* condition, between 300°C and 400°C at 2 GPa (Table S3 in Supporting Information S1). With decreasing f/*r*, the concentrations of dissolved Mg and Al are predicted to increase while concentrations of dissolved Si are predicted to decrease during reaction with DMM and HZ1. During metasomatism of HZ2, concentrations of dissolved Al and Ca are predicted to initially increase and then decrease, while concentrations of dissolved Mg and Si initially decrease then increase with decreasing f/*r* (Figure 1).

Metasomatism of antigorite by fluids that were previously in equilibrium with a metapelite is predicted to form talc coexisting with chlorite + quartz + diaspore at 300°C and 1.5 GPa (Figure S2 in Supporting Information S1). Metasomatism of HZ2 by a metapelite-equilibrated fluid is predicted to yield talc coexisting with chlorite + quartz + antigorite + tremolite at 300°C and 1.5 GPa. Our models suggest that metasomatism of DMM and HZ1 yields chlorite, quartz, clinopyroxene, lawsonite, and diaspore under similar *P-T* condition. If the fluid previously equilibrated with metapelite, the models predict that talc formation is favored during metasomatism of more refractory ultramafic compositions (Table S3 in Supporting Information S1). With decreasing f/*r*, the concentrations of dissolved Si, Ca, and Al are predicted to increase while dissolved Mg decreases (Figure 1).

4. Discussion

4.1. Effects of Fluid and Rock Compositions on Talc Formation

Talc can form during serpentinization, closed-system metamorphism of serpentinite, and metasomatism of ultramafic rocks. Talc formation is favored during low-pressure serpentinization of pyroxene at temperatures of 400°C or higher where olivine is stable in the presence of water (Evans, 1977; Frost & Beard, 2007; Klein et al., 2009). Prograde metamorphism of antigorite can yield olivine, talc, and water whereas retrograde metamorphism of antigorite can form chrysotile and talc (Schwartz et al., 2013). The volume of talc formation during serpentinization or closed-system metamorphism is small when compared with other reaction products. In contrast, the formation of sizable talc deposits, such as those in the exhumed high-pressure terrane on Santa Catalina Island (USA), would require an open-system reaction involving the external addition of silica-bearing fluids into serpentinite (Bebout and Barton, 2002). The formation of talc at the expense of ultramafic rocks can be assessed using the simplified MgO-SiO_2-H_2O (MSH) system (Bowen & Tuttle, 1949; Evans, 1977).

Serpentinization

$$\underset{\text{(orthopyroxene)}}{90\,MgSiO_3} + 45\,H_2O = \underset{\text{(antigorite)}}{Mg_{48}Si_{34}O_{85}(OH)_{62}} + 14\,\underset{\text{(talc)}}{Mg_3Si_4O_{10}(OH)_2} \quad \text{(R1)}$$

Metamorphism

$$\underset{\text{(anthophyllite)}}{5\,Mg_7Si_8O_{22}(OH)_2} + 2\,H_2O = 9\,\underset{\text{(talc)}}{Mg_3Si_4O_{10}(OH)_2} + 4\,\underset{\text{(olivine)}}{Mg_2SiO_4} \quad \text{(R2)}$$

$$\underset{\text{(antigorite)}}{Mg_{48}Si_{34}O_{85}(OH)_{62}} = 18\,\underset{\text{(olivine)}}{Mg_2SiO_4} + 4\,\underset{\text{(talc)}}{Mg_3Si_4O_{10}(OH)_2} + 27\,H_2O \quad \text{(R3)}$$

Si-metasomatism

$$\underset{\text{(olivine)}}{3\,Mg_2SiO_4} + 5\,SiO_{2(aq)} + 2\,H_2O = 2\,\underset{\text{(talc)}}{Mg_3Si_4O_{10}(OH)_2} \quad \text{(R4)}$$

$$\underset{\text{(orthopyroxene)}}{3\,MgSiO_3} + SiO_{2(aq)} + H_2O = \underset{\text{(talc)}}{Mg_3Si_4O_{10}(OH)_2} \quad \text{(R5)}$$

$$\underset{\text{(antigorite)}}{Mg_{48}Si_{34}O_{85}(OH)_{62}} + 30\,SiO_{2(aq)} = 16\,\underset{\text{(talc)}}{Mg_3Si_4O_{10}(OH)_2} + 15\,H_2O \quad \text{(R6)}$$

While serpentinization and metamorphism of serpentinite can proceed without the addition or removal of components, except for water (e.g., R1–R3), the formation of talc may also be favored via the addition of SiO_2 to—or the removal of MgO from—an ultramafic rock. However, factors other than SiO_2 addition and MgO removal need to be considered when assessing the stability of talc, notably the compositions of the reactant rock and fluid, f/*r*, and temperature (Klein et al., 2013).

Our model predictions at 300°C and 1.5 GPa suggest that the reaction of a quartz-saturated fluid with DMM, HZ1, or HZ2 can yield minerals such as chlorite, garnet, clinopyroxene, orthopyroxene, pumpellyite, in addition to talc. The formation of talc is predicted to be more favorable during Si-metasomatism of DMM and HZ1 when compared with HZ2 which we attribute to the higher bulk-rock Al contents and lower Mg/Si ratios in less melt-depleted mantle rocks (Figure S6 in Supporting Information S1). The lower bulk-rock Al contents and higher Mg/Si of more melt-depleted mantle rocks (here HZ2) favor the formation of Al-bearing phases such as chlorite, paragonite, and garnet rather than talc (Figure 2). Si-metasomatism of fertile mantle rocks is predicted to

favor the formation of Ca-bearing phases such as clinopyroxene, lawsonite, and grossular-rich garnet due to their elevated bulk-rock Ca contents relative to refractory harzburgite.

Our models predict that metasomatism of antigorite by fluids that previously equilibrated with metabasalt can favor the formation of chlorite and clinopyroxene, in addition to talc (Figure S2; Table S3 in Supporting Information S1). However, if the fluid equilibrates with metabasalt before reacting with peridotite (DMM, HZ1, and HZ2), talc formation is predicted to occur only between 300°C and 400°C at 2 GPa (Table S3 in Supporting Information S1). A possible explanation is the relatively high Si concentrations and low Mg/Si ratios of the fluid at these conditions when compared with similar temperatures at different pressures. We attribute talc formation during metasomatism of refractory HZ2 peridotite by fluids that previously equilibrated with metapelite with the relatively low bulk-rock Al contents and high Mg/Si ratios, as well as the low dissolved Al content and low Al/Si ratio of the reactant fluid (Table S3; Figures S1 and S6 in Supporting Information S1).

The reaction-path models suggest that the compositions of reacting fluids and whole-rocks at a given *P-T* condition are pivotal in controlling the chemical affinity to form talc. This implies that the formation of talc may be restricted to specific domains where rock and fluid compositions, as well as pressure and temperature are favorable, for example, where sediments and refractory harzburgite are juxtaposed at 300°C–400°C and 1–2 GPa. However, juxtaposition of mafic and ultramafic rocks is predicted to favor the formation of Ca- and Al-bearing phases such as chlorite, clinopyroxene, lawsonite, garnet, epidote, and paragonite over talc. A fluid that is Si-rich but Ca- and Al-poor could produce talc upon reaction with fertile ultramafic compositions; however, such fluid compositions seem unlikely considering the abundance of Ca- and Al-bearing phases in subducting slabs that become unstable during metamorphism.

4.2. Limited Talc Formation Along the Subduction Interface

The thermal structure of subducting slabs is of central importance regarding the *P-T* stability of hydrous minerals. In addition to *P* and *T*, our calculations suggest that rock and fluid compositions should not be ignored when the stability of hydrous minerals in subduction zones is evaluated (Figure 3a). Figure 3b summarizes the conditions where talc formation is predicted relative to distinct slab-top geotherms (Syracuse et al., 2010). As talc formation during Si-metasomatism is favored at relatively low temperatures and pressures, we expect to find more talc in cold subduction zones, such as Izu-Bonin-Mariana and Tonga, than in warm subduction zones such as in Cascadia and Mexico. If this is correct, more extensive talc formation via Si-metasomatism of ultramafic rocks along the slab-mantle interface at subarc depths may be limited to cold subduction zones. We also infer that talc formation at the slab-mantle interface may be limited in subduction zones where sediments are scraped off before subduction or if the sediment layer of the subducting oceanic plate is thin.

Talc-bearing metamorphic rocks from the Arosa Zone (Switzerland) and on Santa Catalina Island (USA) can be used to further evaluate our model predictions. The Arosa Zone exhibits an exhumed plate interface that includes calcareous and pelitic schists, metabasite, marble, serpentinite, and chlorite and talc schists (Condit et al., 2022). Talc schist forms a 2–4 m thick layer between ultramafic and mafic rocks. While the *P-T* conditions of talc and chlorite formation at Arosa are unknown, it is estimated that the latest stage of subduction-related deformation of the region may have occurred at 300°C–350°C and pressures above 0.7 GPa (Bachmann et al., 2009). If we consider this estimate as a minimum bound for talc (and chlorite) formation due to its deformation texture, this would be comparable and consistent with our model prediction where talc can form at temperature ≤400°C at 1 GPa.

On Santa Catalina Island (USA), a talc-bearing metasomatic reaction zone developed between serpentinite and metasediments. The heterogeneous mixture of metamorphosed rocks at Catalina recorded a wide range of *P-T* conditions of between ~200°C and ~700°C and between 0.6 and 1.2 GPa. The talc-bearing metamorphosed rocks in this locality record amphibolite-facies conditions (600°C–700°C). This temperature range is significantly higher than the anticipated temperature range for talc formation based on our model predictions for pressures of less than 2 GPa. However, previous petrologic studies on Catalina have suggested that talc must have formed during or after the exhumation-related, chrysotile-bearing deformation observed in the serpentinite domains (Hirauchi et al., 2020; Hirauchi & Yamaguchi, 2007).

Talc can also form during mineral carbonation of ultramafic rocks (Okamoto et al., 2021). This process can transform a Si-undersaturated peridotite or serpentinite into soapstone (mainly talc and magnesite) or even listvenite

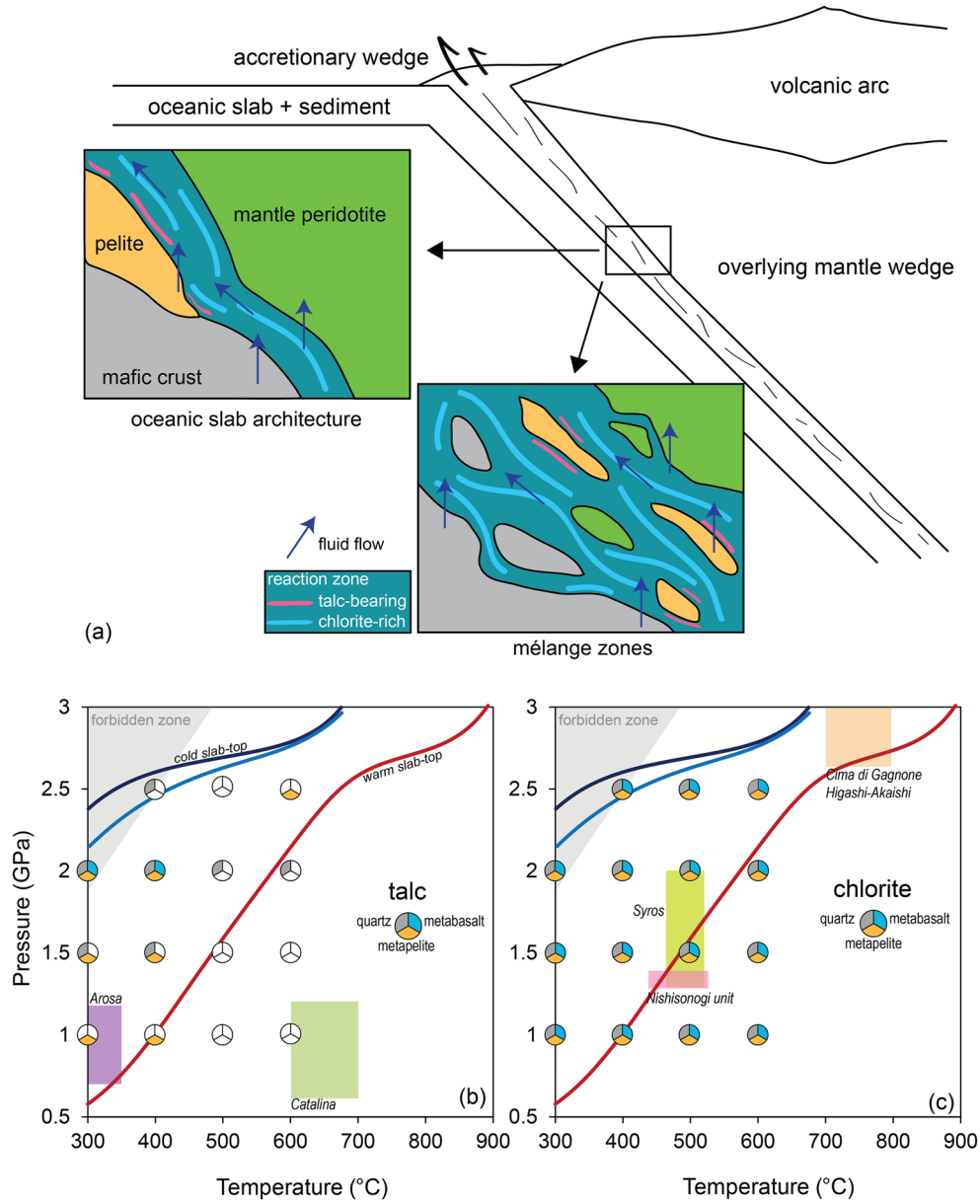

Figure 3. (a) Illustration of the slab-mantle interface in subduction zones where talc and chlorite may be favored to form. Summary of the conditions that are predicted to favor the formation of talc (b) and chlorite (c) via Si-metasomatism of ultramafic rocks by slab-derived fluids. The predicted presence or lack of talc and chlorite is indicated by the color-coded pie charts which refer to distinct fluid compositions used in the reaction path models. The *P-T* conditions of field sites mentioned in the text are shown for comparison. Slab-top geotherms are taken from Syracuse et al. (2010).

(quartz and magnesite) without adding Si, as CO_2 reacts with Mg, Fe, and Ca to form carbonate, allowing Si to react with serpentine to form talc (Grozeva et al., 2017; Klein & Garrido, 2011). While a more detailed account of mineral carbonation is beyond the scope of this study, talc formation through this process may be most effective in subduction zones where the incoming plates carry large volumes of carbonate rocks, such as in the Aegean arc (Clift & Vannucchi, 2004).

4.3. Formation of Chlorite Along the Subduction Interface

Chlorite is predicted to form in almost all of our reaction path models (Figure 3c). The elevated activity of Al species in fluids in equilibrium with metabasalt or metapelite with increasing temperature promotes the

formation of chlorite upon reaction with ultramafic rocks. The increased solubility of Al in fluids with increasing temperature is facilitated by the formation of Al-complexes, such as $Al(OH)Si(OH)^-$ (Huang & Sverjensky, 2019; Manning, 2018). The predicted formation of chlorite is corroborated by the common occurrence of chlorite at the interface between juxtaposed mafic, pelitic, and ultramafic rocks in metamorphic terranes that record a wide range of *P-T* conditions (Bebout, 1991; Bebout & Penniston-Dorland, 2016; Marschall & Schumacher, 2012). Here, Si-metasomatism of ultramafic rocks or Mg-metasomatism of mafic (or pelitic) rocks can yield chlorite-rich assemblages.

Examples of exhumed chlorite-bearing high-pressure rocks with well-constrained *P-T* histories support our model predictions (Figure 2c). The exhumed high-pressure mélange in Syros (Greece), metamorphosed at 1.3–2.0 GPa and 470°C–520°C (Breeding et al., 2004; Marschall et al., 2006), displays chlorite-rich reaction zone between mafic blocks and serpentinite matrix where serpentinite is altered to chlorite ± talc ± tremolite (Gyomlai et al., 2021). Similarly, the ultramafic mélange from the Nishisonogi (Japan), metamorphosed at ∼1.3–1.4 GPa and ∼440°C–520°C (Mori et al., 2019; Moribe, 2013), consists of a matrix of chlorite-actinolite schists and serpentinite juxtaposed to metapelite (Mori et al., 2014). In addition, chlorite and amphibole-rich reaction rinds around mafic blocks on Santa Catalina Island (USA) display elevated MgO, Ni, Cr, Os, Ir and Ru, reflecting ultramafic protoliths (Bebout and Barton, 2002; Penniston-Dorland et al., 2014). Other examples of exhumed mantle wedge peridotite metasomatized by slab-derived fluids include the Higashi-Akaishi peridotite (Japan) and chlorite harzburgites in Cima di Gagnone (Switzerland). These exhumed metaperidotites record peak *P-T* conditions of ∼700°C–800°C and <3 GPa (Guild et al., 2020; Scambelluri et al., 2014). Metasomatism of these metaperidotites by slab-derived fluids may have occurred at or before the rocks had reached peak-metamorphic temperatures. In the Higashi-Akaishi peridotite, high-Mg chlorite and amphibole included within garnet and orthopyroxene were interpreted as a stable prograde assemblage (Enami et al., 2004; Hattori et al., 2010). At Cima di Gagnone, chlorite harzburgite lenses are embedded within metamorphosed pelite. These chlorite harzburgite lenses record enrichments in radiogenic Sr and Pb from the interactions with fluids derived from the enclosing metapelite (Cannaò et al., 2015; Scambelluri et al., 2014). Evidence for chlorite formation and stabilization in mantle rocks by slab-derived fluids is also found in multiphase inclusions in exhumed metaperidotite (Campione et al., 2017). For instance, primary mineral inclusions in mantle garnet from exhumed ultra-high-pressure peridotite (e.g., Maowu Ultramafic Complex in Eastern China, Bardane, Ugelvik and Svartberget in the Western Gneiss Region) include spinel + chlorite which were interpreted as crystallization products of dilute slab-derived aqueous fluids that percolated through mantle peridotites (Campione et al., 2017; Carswell and van Roermund, 2005; Malaspina et al., 2006; Van Roermund & Drury, 1998; Vrijmoed et al., 2008).

4.4. Implications for the Rheology, Slow Slip, and Coupling-Decoupling Transition of the Slab-Mantle Interface

The structurally complex shear zones in subduction interface exposures preserve a mixture of rock types that vary strongly in their rheological properties (Agard et al., 2018). Previous studies have suggested that episodic slip occurs downdip of the seismogenic zone along the plate interface, where the brittle-ductile transition occurs (Audet & Kim, 2016; Bürgmann, 2018). Slow slip occurs over longer timescales and at lower slip rates than seismic ruptures but are episodic and faster than continuous aseismic creep (Beroza & Ide, 2011; Rogers & Dragert, 2003). Slow slip events are typically observed in warm subduction zones at conditions of very low shear stresses (<1 MPa) (Beroza & Ide, 2011; Hawthorne & Rubin, 2010). Their distributions vary between subduction zones, but the majority are found at an inferred depth range of 30–50 km and temperatures between 325°C and 500°C (Brown et al., 2009; Condit et al., 2020). However, the exact mechanisms and conditions controlling their occurrence remain debated (Behr & Bürgmann, 2021). Proposed mechanisms include high pore fluid pressure that may promote dilatant hardening (Segall et al., 2006) or by changing strain partitioning among different rock units (French & Condit, 2019). These fluids are believed to be generated by in-situ dehydration of subducting slab or updip flow of fluids sourced from portions of the subducted slabs that dehydrate at greater depths (Condit et al., 2020; Fagereng et al., 2017; Kodaira et al., 2004; Taetz et al., 2018). The latter mechanism, proposed in conjunction with high pore-fluid pressures, invokes the presence of weak minerals such as chlorite and talc (Condit et al., 2022; French & Condit, 2019; Hirauchi et al., 2020; Tarling et al., 2019). For instance, French and Condit (2019) suggested that the very low shear stresses determined for during slow slip events can be accommodated by frictional deformation of chlorite or talc at near-lithostatic pore-fluid pressures. This is particularly

important as near-lithostatic fluid pressures have been inferred for the plate interface (Behr & Bürgmann, 2021; Condit & French, 2022; Furukawa, 1993).

This study provides additional constraints on strain localization and the potential link to slow slip events by illuminating the formation potential of talc and chlorite along the plate interface. Talc formation via Si-metasomatism may not be as pervasive as previously thought, because it is predicted to form at a restrictive set of conditions only. When fluid in equilibrium with metapelite reacts with an ultramafic rock, talc formation is predicted to be less favorable at temperatures above 400°C at pressures below 2 GPa. If slow slip events depend on the presence and rheological properties of talc at near-lithostatic fluid pressures, then these events would be more favored in subduction zones with cold slab-top geotherms and where the incoming plates contain abundant sediments. However, this is inconsistent with the common occurrence of slow slip events in warm subduction zones such as in Cascadia and Mexico where the incoming plates are sediment-poor (Clift & Vannucchi, 2004). The absence of large volumes of talc in exhumed high-pressure rocks that record peak pressures above 1 GPa, in conjunction with our model predictions (that cover *P-T* conditions that are not represented by the exhumed metamorphic rock record), tentatively suggest that talc formation via Si-metasomatism is less favorable in warm subduction zones than in cold ones. Therefore, talc formed during Si-metasomatism may be less important in promoting of slow slip events in warm subduction zones than previously thought (French & Condit, 2019).

The pressure-dependent breakdown of talc via the reaction with forsterite to form antigorite and enstatite has been suggested as a mechanism to explain the coupling of the slab and overlying mantle at ~80 km depth (S. M. Peacock and Wang, 2021). If our predictions are correct, the common decoupling-coupling transition along the plate interface in warm subduction zones would be difficult to explain with the breakdown of talc, since its formation via Si-metasomatism seems to be limited to a restricted set of environmental conditions. Alternatively, much of the talc may form via mineral carbonation rather than Si-metasomatism (Okamoto et al., 2021).

Since chlorite also displays low frictional strength (Fagereng & Ikari, 2020), its formation along the plate interface largely independent of the slab thermal structure may be more likely to facilitate strain localization and facilitate slow slip events when the pore fluid pressure approaches lithostatic condition. However, other processes or mechanisms are required for chlorite to host slow slips at depths where they are generated.

Downdip of the brittle-ductile transition, increasing temperature in the presence of fluids may further promote the metasomatic growth of chlorite at the expense of precursor rocks. This would promote decoupling and possibly the deepening of the decoupling-coupling transition of the plate interface over time (cf. Abers et al., 2020; Marschall & Schumacher, 2012).

Data Availability Statement

The data that support the findings of this study are freely available at https://doi.org/10.5281/zenodo.6760195. The Deep Earth Water (DEW) database and EQ3/6 thermodynamic codes are available online (http://www.dewcommunity.org/resources.html).

Acknowledgments
This work was support by National Science Foundation Award # 1545903 (PIRE: ExTerra Field Institute and Research Endeavour), and the WHOI Ocean Ventures Fund.

References

Abers, G. A., van Keken, P. E., & Wilson, C. R. (2020). Deep decoupling in subduction zones: Observations and temperature limits. *Geosphere*, *16*(6), 1408–1424. https://doi.org/10.1130/GES02278.1

Agard, P., Plunder, A., Angiboust, S., Bonnet, G., & Ruh, J. (2018). The subduction plate interface: Rock record and mechanical coupling (from long to short timescales). *Lithos*, *320–321*, 537–566. https://doi.org/10.1016/j.lithos.2018.09.029

Ague, J. J. (2007). Models of permeability contrasts in subduction zone mélange: Implications for gradients in fluid fluxes, Syros and Tinos Islands, Greece. *Chemical Geology*, *239*(3–4), 217–227. https://doi.org/10.1016/j.chemgeo.2006.08.012

Audet, P., & Kim, Y. (2016). Teleseismic constraints on the geological environment of deep episodic slow earthquakes in subduction zone forearcs: A review. *Tectonophysics*, *670*, 1–15. https://doi.org/10.1016/j.tecto.2016.01.005

Bachmann, R., Oncken, O., Glodny, J., Seifert, W., Georgieva, V., & Sudo, M. (2009). Exposed plate interface in the European Alps reveals fabric styles and gradients related to an ancient seismogenic coupling zone. *Journal of Geophysical Research*, *114*(B5), B05402. https://doi.org/10.1029/2008JB005927

Bebout, G. (2013). Metasomatism in subduction zones of subducted oceanic slabs, mantle wedges, and the slab-mantle interface. In *Metasomatism and the chemical transformation of rock* (pp. 289–349). https://doi.org/10.1007/978-3-642-28394-9_9

Bebout, G. E. (1991). Field-based evidence for devolatilization in subduction zones: Implications for arc magmatism. *Science*, *251*(4992), 413–416. https://doi.org/10.1126/science.251.4992.413

Bebout, G. E., & Barton, M. D. (2002). Tectonic and metasomatic mixing in a high-T, subduction-zone mélange—Insights into the geochemical evolution of the slab–mantle interface. *Chemical Geology*, *187*(1–2), 79–106. https://doi.org/10.1016/S0009-2541(02)00019-0

Bebout, G. E., & Penniston-Dorland, S. C. (2016). Fluid and mass transfer at subduction interfaces—The field metamorphic record. *Lithos*, *240–243*, 228–258. https://doi.org/10.1016/j.lithos.2015.10.007

Behr, W. M., & Bürgmann, R. (2021). What's down there? The structures, materials and environment of deep-seated slow slip and tremor. *Philosophical Transactions of the Royal Society A: Mathematical, Physical & Engineering Sciences*, *379*(2193), 20200218. https://doi.org/10.1098/rsta.2020.0218

Beroza, G. C., & Ide, S. (2011). Slow earthquakes and nonvolcanic tremor. *Annual Review of Earth and Planetary Sciences*, *39*(1), 271–296. https://doi.org/10.1146/annurev-earth-040809-152531

Boschi, C., Fruh-Green, G., & Escartin, J. (2006). 31—occurrence and significance of serpentinite-hosted, talc-rich fault rocks in modern oceanic settings and ophiolite complexes. *Ofioliti*, *31*, 141–150.

Bose, K., & Ganguly, J. (1995). Experimental and theoretical studies of the stabilities of talc, antigorite and phase A at high pressures with applications to subduction processes. *Earth and Planetary Science Letters*, *136*(3–4), 109–121. https://doi.org/10.1016/0012-821X(95)00188-I

Bowen, N. L., & Tuttle, O. F. (1949). The system MgO–SiO_2–H_2O. *GSA Bulletin*, *60*(3), 439–460. https://doi.org/10.1130/0016-7606(1949)60[439:TSM]2.0.CO;2

Breeding, C. M., Ague, J. J., & Bröcker, M. (2004). Fluid–metasedimentary rock interactions in subduction-zone mélange: Implications for the chemical composition of arc magmas. *Geology*, *32*(12), 1041–1044. https://doi.org/10.1130/G20877.1

Brown, J. R., Beroza, G. C., Ide, S., Ohta, K., Shelly, D. R., Schwartz, S. Y., et al. (2009). Deep low-frequency earthquakes in tremor localize to the plate interface in multiple subduction zones. *Geophysical Research Letters*, *36*(19), L19306. https://doi.org/10.1029/2009GL040027

Bürgmann, R. (2018). The geophysics, geology and mechanics of slow fault slip. *Earth and Planetary Science Letters*, *495*, 112–134. https://doi.org/10.1016/j.epsl.2018.04.062

Campione, M., Tumiati, S., & Malaspina, N. (2017). Primary spinel + chlorite inclusions in mantle garnet formed at ultrahigh-pressure. *Geochemical Perspectives Letters*, *4*, 19–23. https://doi.org/10.7185/geochemlet.1730

Cannaò, E., Agostini, S., Scambelluri, M., Tonarini, S., & Godard, M. (2015). B, Sr and Pb isotope geochemistry of high-pressure Alpine metaperidotites monitors fluid-mediated element recycling during serpentinite dehydration in subduction mélange (Cima di Gagnone, Swiss Central Alps). *Geochimica et Cosmochimica Acta*, *163*, 80–100. https://doi.org/10.1016/j.gca.2015.04.024

Carswell, D. A., & van Roermund, H. L. M. (2005). On multi-phase mineral inclusions associated with microdiamond formation in mantle-derived peridotite lens at Bardane on Fjørtoft, west Norway. *European Journal of Mineralogy*, *17*(1), 31–42. https://doi.org/10.1127/0935-1221/2005/0017-0031

Chen, X., Elwood Madden, A., & Reches, Z. (2017). The frictional strength of talc gouge in high-velocity shear experiments: Frictional strength of talc gouge. *Journal of Geophysical Research: Solid Earth*, *122*(5), 3661–3676. https://doi.org/10.1002/2016JB013676

Clift, P., & Vannucchi, P. (2004). Controls on tectonic accretion versus erosion in subduction zones: Implications for the origin and recycling of the continental crust. *Reviews of Geophysics*, *42*(2). https://doi.org/10.1029/2003RG000127

Codillo, E. (2022). Thermodynamic constraints on Si-metasomatism of ultramafic rocks in subduction zones. https://doi.org/10.5281/zenodo.6760195

Condit, C. B., & French, M. E. (2022). Geologic evidence of lithostatic pore fluid pressures the base of the subduction seismogenic zone. *Geophysical Research Letters*, *49*(12), e2022GL098862. https://doi.org/10.1029/2022GL098862

Condit, C. B., French, M. E., Hayles, J. A., Yeung, L. Y., Chin, E. J., & Lee, C.-T. A. (2022). Rheology of metasedimentary rocks at the base of the subduction seismogenic zone. *Geochemistry, Geophysics, Geosystems*, *23*(2), e2021GC010194. https://doi.org/10.1029/2021GC010194

Condit, C. B., Guevara, V. E., Delph, J. R., & French, M. E. (2020). Slab dehydration in warm subduction zones at depths of episodic slip and tremor. *Earth and Planetary Science Letters*, *552*, 116601. https://doi.org/10.1016/j.epsl.2020.116601

Enami, M., Mizukami, T., & Yokoyama, K. (2004). Metamorphic evolution of garnet-bearing ultramafic rocks from the Gongen area, Sanbagawa belt, Japan. *Journal of Metamorphic Geology*, *22*, 1–15. https://doi.org/10.1111/j.1525-1314.2003.00492.x

Evans, B. W. (1977). Metamorphism of alpine peridotite and serpentinite. *Annual Review of Earth and Planetary Sciences*, *5*(1), 397–447. https://doi.org/10.1146/annurev.ea.05.050177.002145

Fagereng, Å., Diener, J. F. A., Meneghini, F., Harris, C., & Kvadsheim, A. (2017). Quartz vein formation by local dehydration embrittlement along the deep, tremorgenic subduction thrust interface. *Geology*, *46*(1), 67–70. https://doi.org/10.1130/G39649.1

Fagereng, Å., & Ikari, M. J. (2020). Low-temperature frictional characteristics of chlorite-epidote-amphibole assemblages: Implications for strength and seismic style of retrograde fault zones. *Journal of Geophysical Research: Solid Earth*, *125*(4), e2020JB019487. https://doi.org/10.1029/2020JB019487

French, M. E., & Condit, C. B. (2019). Slip partitioning along an idealized subduction plate boundary at deep slow slip conditions. *Earth and Planetary Science Letters*, *528*, 115828. https://doi.org/10.1016/j.epsl.2019.115828

Frost, B. R., & Beard, J. S. (2007). On silica activity and serpentinization. *Journal of Petrology*, *48*(7), 1351–1368. https://doi.org/10.1093/petrology/egm021

Furukawa, Y. (1993). Depth of the decoupling plate interface and thermal structure under arcs. *Journal of Geophysical Research*, *98*(B11), 20005–20013. https://doi.org/10.1029/93JB02020

Grozeva, N. G., Klein, F., Seewald, J. S., & Sylva, S. P. (2017). Experimental study of carbonate formation in oceanic peridotite. *Geochimica et Cosmochimica Acta*, *199*, 264–286. https://doi.org/10.1016/j.gca.2016.10.052

Guild, M. R., Till, C. B., Mizukami, T., & Wallis, S. (2020). Petrogenesis of the Higashi-Akaishi ultramafic body: Implications for lower crustal foundering and mantle wedge processes. *Journal of Petrology*, *61*(9), egaa089. https://doi.org/10.1093/petrology/egaa089

Gyomlai, T., Agard, P., Marschall, H. R., Jolivet, L., & Gerdes, A. (2021). Metasomatism and deformation of block-in-matrix structures in Syros: The role of inheritance and fluid-rock interactions along the subduction interface. *Lithos*, *386–387*, 386105996–386106387. https://doi.org/10.1016/j.lithos.2021.105996

Hacker, B. R., Abers, G. A., & Peacock, S. M. (2003). Subduction factory 1. Theoretical mineralogy, densities, seismic wave speeds, and H_2O contents. *Journal of Geophysical Research*, *108*(B1). https://doi.org/10.1029/2001JB001127

Hattori, K., Wallis, S., Enami, M., & Mizukami, T. (2010). Subduction of mantle wedge peridotites: Evidence from the Higashi-Akaishi ultramafic body in the Sanbagawa metamorphic belt. *Island Arc*, *19*(1), 192–207. https://doi.org/10.1111/j.1440-1738.2009.00696.x

Hawthorne, J. C., & Rubin, A. M. (2010). Tidal modulation of slow slip in Cascadia. *Journal of Geophysical Research*, *115*(B9), B09406. https://doi.org/10.1029/2010JB007502

Helgeson, H. C., Kirkham, D. H., & Flowers, G. C. (1981). Theoretical prediction of the thermodynamic behavior of aqueous electrolytes by high pressures and temperatures; IV, Calculation of activity coefficients, osmotic coefficients, and apparent molal and standard and relative partial molal properties to 600 degrees C and 5 kb. *American Journal of Science*, *281*(10), 1249–1516. https://doi.org/10.2475/ajs.281.10.1249

Hirauchi, K., den Hartog, S. A. M., & Spiers, C. J. (2013). Weakening of the slab–mantle wedge interface induced by metasomatic growth of talc. *Geology*, *41*(1), 75–78. https://doi.org/10.1130/G33552.1

Hirauchi, K., & Yamaguchi, H. (2007). Unique deformation processes involving the recrystallization of chrysotile within serpentinite: Implications for aseismic slip events within subduction zones. *Terra Nova*, *19*(6), 454–461. https://doi.org/10.1111/j.1365-3121.2007.00771.x

Hirauchi, K., Yamamoto, Y., den Hartog, S. A. M., & Niemeijer, A. R. (2020). The role of metasomatic alteration on frictional properties of subduction thrusts: An example from a serpentinite body in the Franciscan Complex, California. *Earth and Planetary Science Letters*, *531*, 115967. https://doi.org/10.1016/j.epsl.2019.115967

Huang, F., & Sverjensky, D. A. (2019). Extended Deep Earth Water Model for predicting major element mantle metasomatism. *Geochimica et Cosmochimica Acta*, *254*, 192–230. https://doi.org/10.1016/j.gca.2019.03.027

Kim, Y., Clayton, R. W., Asimow, P. D., & Jackson, J. M. (2013). Generation of talc in the mantle wedge and its role in subduction dynamics in central Mexico. *Earth and Planetary Science Letters*, *384*, 81–87. https://doi.org/10.1016/j.epsl.2013.10.006

Klein, F., Bach, W., Jöns, N., McCollom, T., Moskowitz, B., & Berquó, T. (2009). Iron partitioning and hydrogen generation during serpentinization of abyssal peridotites from 15°N on the Mid-Atlantic Ridge. *Geochimica et Cosmochimica Acta*, *73*(22), 6868–6893. https://doi.org/10.1016/j.gca.2009.08.021

Klein, F., Bach, W., & McCollom, T. M. (2013). Compositional controls on hydrogen generation during serpentinization of ultramafic rocks. *Lithos*, *178*, 55–69. https://doi.org/10.1016/j.lithos.2013.03.008

Klein, F., & Garrido, C. J. (2011). Thermodynamic constraints on mineral carbonation of serpentinized peridotite. *Lithos*, *126*(3–4), 147–160. https://doi.org/10.1016/j.lithos.2011.07.020

Kodaira, S., Iidaka, T., Kato, A., Park, J.-O., Iwasaki, T., & Kaneda, Y. (2004). High pore fluid pressure may cause silent slip in the Nankai trough. *Science*, *304*(5675), 1295–1298. https://doi.org/10.1126/science.1096535

Malaspina, N., Hermann, J., Scambelluri, M., & Compagnoni, R. (2006). Polyphase inclusions in garnet–orthopyroxenite (Dabie Shan, China) as monitors for metasomatism and fluid-related trace element transfer in subduction zone peridotite. *Earth and Planetary Science Letters*, *249*(3–4), 173–187. https://doi.org/10.1016/j.epsl.2006.07.017

Manning, C. (2007). Solubility of corundum + kyanite in H_2O at 700°C and 10 kbar: Evidence for Al_Si complexing at high pressure and temperature. *Geofluids*, *7*(2), 258–269. https://doi.org/10.1111/j.1468-8123.2007.00179.x

Manning, C. E. (1995). Phase-equilibrium controls on SiO_2 metasomatism by aqueous fluid in subduction zones: Reaction at constant pressure and temperature. *International Geology Review*, *37*(12), 1074–1093. https://doi.org/10.1080/00206819509465440

Manning, C. E. (1997). Coupled reaction and flow in subduction zones: Silica metasomatism in the mantle wedge. In B. Jamtveit & B. W. D. Yardley (Eds.), *Fluid flow and transport in rocks: Mechanisms and effects* (pp. 139–148). Springer Netherlands. https://doi.org/10.1007/978-94-009-1533-6_8

Manning, C. E. (2004). The chemistry of subduction-zone fluids. *Earth and Planetary Science Letters*, *223*(1–2), 1–16. https://doi.org/10.1016/j.epsl.2004.04.030

Manning, C. E. (2018). Fluids of the lower crust: Deep is different. *Annual Review of Earth and Planetary Sciences*, *46*(1), 67–97. https://doi.org/10.1146/annurev-earth-060614-105224

Marschall, H. R., Ludwid, T., Altherr, R., Kalt, A., & Tonarini, S. (2006). Syros metasomatic Tourmaline: Evidence for very high-δ^{11}B fluids in subduction zones. *Journal of Petrology*, *47*(10), 1915–1942. https://doi.org/10.1093/petrology/egl031

Marschall, H. R., & Schumacher, J. C. (2012). Arc magmas sourced from mélange diapirs in subduction zones. *Nature Geoscience*, *5*(12), 862–867. https://doi.org/10.1038/ngeo1634

Moore, D. E., & Lockner, D. A. (2007). Comparative deformation behavior of minerals in serpentinized ultramafic rock: Application to the slab-mantle interface in subduction zones. *International Geology Review*, *49*(5), 401–415. https://doi.org/10.2747/0020-6814.49.5.401

Mori, Y., Shigeno, M., Miyazaki, K., & Nishiyama, T. (2019). Peak metamorphic temperature of the Nishisonogi unit of the Nagasaki metamorphic rocks, Western Kyushu, Japan. *Journal of Mineralogical and Petrological Sciences*, *114*(4), 170–177. https://doi.org/10.2465/jmps.190423

Mori, Y., Shigeno, M., & Nishiyama, T. (2014). Fluid-metapelite interaction in an ultramafic mélange: Implications for mass transfer along the slab-mantle interface in subduction zones. *Earth Planets and Space*, *66*(1), 47. https://doi.org/10.1186/1880-5981-66-47

Moribe, Y. (2013). *Petrological study of the Nagasaki metamorphic rocks in the Nishisonogi Peninsula, western Kyusyu. Master's thesis*. Kumamoto University.

Okamoto, A., Oyanagi, R., Yoshida, K., Uno, M., Shimizu, H., & Satish-Kumar, M. (2021). Rupture of wet mantle wedge by self-promoting carbonation. *Communications Earth & Environment*, *2*(1), 151. https://doi.org/10.1038/s43247-021-00224-5

Peacock, S. (1990). Fluid processes in subduction zones. *Science*, *248*(4953), 329–337. https://doi.org/10.1126/science.248.4953.329

Peacock, S. M., & Hyndman, R. D. (1999). Hydrous minerals in the mantle wedge and the maximum depth of subduction thrust earthquakes. *Geophysical Research Letters*, *26*(16), 2517–2520. https://doi.org/10.1029/1999GL900558

Peacock, S. M., & Wang, K. (2021). On the stability of talc in subduction zones: A possible control on the maximum depth of decoupling between the subducting plate and mantle wedge. *Geophysical Research Letters*, *48*(17), e2021GL094889. https://doi.org/10.1029/2021GL094889

Penniston-Dorland, S. C., Gorman, J. K., Bebout, G. E., Piccoli, P. M., & Walker, R. J. (2014). Reaction rind formation in the Catalina Schist: Deciphering a history of mechanical mixing and metasomatic alteration. *Chemical Geology*, *384*, 47–61. https://doi.org/10.1016/j.chemgeo.2014.06.024

Rogers, G., & Dragert, H. (2003). Episodic tremor and slip on the Cascadia subduction zone: The chatter of silent slip. *Science*, *300*(5627), 1942–1943. https://doi.org/10.1126/science.1084783

Rubin, A. M. (2008). Episodic slow slip events and rate-and-state friction. *Journal of Geophysical Research*, *113*(B11), B11414. https://doi.org/10.1029/2008JB005642

Scambelluri, M., Pettke, T., Rampone, E., Godard, M., & Reusser, E. (2014). Petrology and trace element budgets of high-pressure peridotites indicate subduction dehydration of serpentinized mantle (Cima di Gagnone, Central Alps, Switzerland). *Journal of Petrology*, *55*(3), 459–498. https://doi.org/10.1093/petrology/egt068

Schwartz, S., Guillot, S., Reynard, B., Lafay, R., Debret, B., Nicollet, C., et al. (2013). Pressure–temperature estimates of the lizardite/antigorite transition in high pressure serpentinites. *Lithos*, *178*, 197–210. https://doi.org/10.1016/j.lithos.2012.11.023

Segall, P., Desmarais, E. K., Shelly, D., Miklius, A., & Cervelli, P. (2006). Earthquakes triggered by silent slip events on Kīlauea volcano, Hawaii. *Nature*, *442*(7098), 71–74. https://doi.org/10.1038/nature04938

Shock, E. L., Oelkers, E. H., Johnson, J. W., Sverjensky, D. A., & Helgeson, H. C. (1992). Calculation of the thermodynamic properties of aqueous species at high pressures and temperatures. Effective electrostatic radii, dissociation constants and standard partial molal properties to 1000°C and 5 kbar. *Journal of the Chemical Society*, *88*(6), 803–826. https://doi.org/10.1039/ft9928800803

Sverjensky, D. A. (2019). Thermodynamic modelling of fluids from surficial to mantle conditions. *Journal of the Geological Society*, *176*(2), 348–374. https://doi.org/10.1144/jgs2018-105

Sverjensky, D. A., Harrison, B., & Azzolini, D. (2014). Water in the deep Earth: The dielectric constant and the solubilities of quartz and corundum to 60kb and 1200°C. *Geochimica et Cosmochimica Acta*, *129*, 125–145. https://doi.org/10.1016/j.gca.2013.12.019

Syracuse, E. M., van Keken, P. E., & Abers, G. A. (2010). The global range of subduction zone thermal models. *Physics of the Earth and Planetary Interiors*, *183*(1–2), 73–90. https://doi.org/10.1016/j.pepi.2010.02.004

Taetz, S., John, T., Bröcker, M., Spandler, C., & Stracke, A. (2018). Fast intraslab fluid-flow events linked to pulses of high pore fluid pressure at the subducted plate interface. *Earth and Planetary Science Letters*, *482*, 33–43. https://doi.org/10.1016/j.epsl.2017.10.044

Tarling, M. S., Smith, S. A. F., & Scott, J. M. (2019). Fluid overpressure from chemical reactions in serpentinite within the source region of deep episodic tremor. *Nature Geoscience*, *12*(12), 1034–1042. https://doi.org/10.1038/s41561-019-0470-z

Van Roermund, D., & Drury (1998). Ultra-high pressure (P > 6 GPa) garnet peridotites in Western Norway: Exhumation of mantle rocks from >185 km depth. *Terra Nova*, *10*, 295–301. https://doi.org/10.1046/j.1365-3121.1998.00213.x

Vrijmoed, J. C., Smith, D. C., & Van Roermund, H. L. M. (2008). Raman confirmation of microdiamond in the Svartberget Fe-Ti type garnet peridotite, Western Gneiss Region, Western Norway. *Terra Nova*, *20*(4), 295–301. https://doi.org/10.1111/j.1365-3121.2008.00820.x

Wada, I., Wang, K., He, J., & Hyndman, R. D. (2008). Weakening of the subduction interface and its effects on surface heat flow, slab dehydration, and mantle wedge serpentinization. *Journal of Geophysical Research*, *113*(B4), B04402. https://doi.org/10.1029/2007JB005190

Whitney, D. L., & Evans, B. W. (2010). Abbreviations for names of rock-forming minerals. *American Mineralogist*, *95*(1), 185–187. https://doi.org/10.2138/am.2010.3371

Wolery, T. J. (1992). EQ3/6, a software package for geochemical modeling of aqueous systems: Package overview and installation guide (version 7.0). https://doi.org/10.2172/138894

References From the Supporting Information

Deschamps, F., Godard, M., Guillot, S., & Hattori, K. (2013). Geochemistry of subduction zone serpentinites: A review. *Lithos*, *178*, 96–127. https://doi.org/10.1016/j.lithos.2013.05.019

Helgeson, H. C. (1969). Thermodynamics of hydrothermal systems at elevated temperatures and pressures. *American Journal of Science*, *267*(7), 729–804. https://doi.org/10.2475/ajs.267.7.729

Kessel, R., Schmidt, M. W., Ulmer, P., & Pettke, T. (2005). Trace element signature of subduction-zone fluids, melts and supercritical liquids at 120–180 km depth. *Nature*, *437*(7059), 724–727. https://doi.org/10.1038/nature03971

Le Roux, V., Bodinier, J.-L., Tommasi, A., Alard, O., Dautria, J., Vauchez, A., & Riches, A. (2007). The Lherz spinel lherzolite: Refertilized rather than pristine mantle. *Earth and Planetary Science Letters*, *259*(3–4), 599–612. https://doi.org/10.1016/j.epsl.2007.05.026

Wei, C., & Powell, R. (2004). Calculated phase relations in high-pressure metapelites in the system NKFMASH (Na_2O–K_2O–FeO–MgO–Al_2O_3–SiO_2–H_2O). *Journal of Petrology*, *45*(1), 183–202. https://doi.org/10.1093/petrology/egg085

Workman, R. K., & Hart, S. R. (2005). Major and trace element composition of the depleted MORB mantle (DMM). *Earth and Planetary Science Letters*, *231*(1–2), 53–72. https://doi.org/10.1016/j.epsl.2004.12.005

Zhang, Z., & Duan, Z. (2005). Prediction of the PVT properties of water over wide range of temperatures and pressures from molecular dynamics simulation. *Physics of the Earth and Planetary Interiors*, *149*(3–4), 335–354. https://doi.org/10.1016/j.pepi.2004.11.003